

# The ATLAS Muon Spectrometer

---

**Koji ISHII\***, on behalf of the ATLAS Muon group

*Graduate School of Science and Technology, KOBE University, Kobe Hyogo 657, Japan*

*E-mail: ishii@phys.sci.kobe-u.ac.jp*

**ABSTRACT:** The LHC experiments will start in April 2006. The ATLAS detector, one of the general purpose detectors, is now under construction. The ATLAS Muon Spectrometer employs three large air-core superconducting toroid magnets, and dedicated chambers for tracking and triggering. The Monitored Drift Tubes (MDTs) provide precision measurements of muon tracks over most of the pseudo-rapidity range. The Resistive Plate Chambers (RPCs) in the barrel and the Thin Gap Chambers (TGCs) in the end-caps generate trigger signals with bunch crossing identification. This report presents the components designs, production status and quality controls, along with the design and development status of the ATLAS muon trigger system.

---

## 1. Introduction

The LHC experiments have a rich physics potential, discovery of new particles such as Higgs bosons and supersymmetric partners, and high accuracy measurements of quarks and gauge bosons. To maximize these potentials the ATLAS detector has been designed. The major requirements for the ATLAS Muon Spectrometer follow [1].

- The momentum resolution of a reconstructed muon track should be better than 2 % for the transverse momentum ( $P_T$ ) of 5 to 100 GeV. This is an essential requirement for the mass reconstruction of narrow two and four muon final states, such as the intermediated or heavy mass Higgs.
- Trigger selectivity is needed to cover a wide range of topics. The high- $P_T$  threshold of about 20 GeV is adequate for LHC physics with a high mass state. The low- $P_T$  threshold of about 6 GeV is required for the CP violation and B physics.
- Second-coordinate measurements with around 10 mm spatial resolution are required for the track reconstruction.

---

\*Speaker.

- The time resolution should be better than the LHC bunch spacing of 25 ns.

We designed the ATLAS Muon Spectrometer as a stand-alone system [2]. We use air-core superconducting toroid magnets, which cover a large rapidity range and minimize multiple scattering. To achieve both good momentum resolution of muon tracks and good time resolution for the first level trigger system, dedicated chambers for tracking and triggering are provided. Four different types of gaseous chambers are employed.

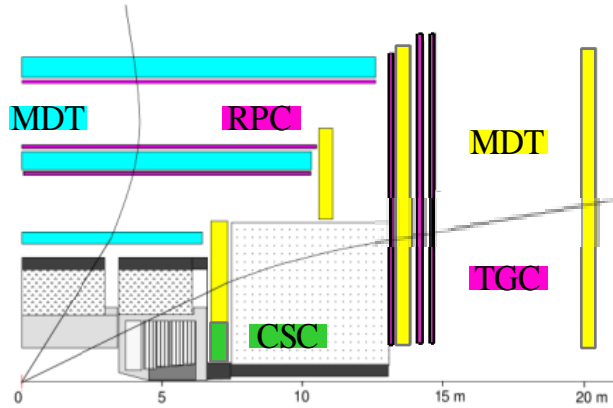


**Figure 1:** The ATLAS muon detectors.

Figure 1 shows a layout of the ATLAS muon detectors. For precision measurements of muon tracks in the principle bending direction of the magnetic field, Monitored Drift Tubes (MDTs) are used. A tube can achieve a single wire resolution of approximately  $80 \mu\text{m}$  with robust and reliable operation thanks to its mechanical isolation from neighboring wires. The MDTs cover the pseudorapidity range of  $|\eta| < 2$ . In the barrel region, the MDTs are arranged in three cylindrical stations around the beam axis. In the end-cap regions, the MDTs are installed vertically, also in three stations. At large pseudorapidity and close to the beam axis, where particle fluxes are highest, the Cathode Strip Chambers (CSCs) are used over  $2 < |\eta| < 2.7$ . The trigger system covers the pseudorapidity range of  $|\eta| < 2.4$ . The trigger function in the barrel is provided by three stations of Resistive Plate Chambers (RPCs), which have a good space time resolution of typically  $1 \text{ cm} \times 1 \text{ ns}$ . They are located on both sides of the middle MDT station and directly inside the outer station. Three stations of Thin Gap Chambers (TGCs) give the end-cap trigger, where particle fluxes are higher than in the barrel. The TGCs are located near the middle MDT station. The RPCs and TGCs also provide the second-coordinate measurements.

Table 1 summarizes the number of chambers, channels, and the area covered for the four chamber technologies. A large number of chambers need to be built and installed for the ATLAS detector. To meet the first collision a strict production schedule is programmed. Quality controls are also important issues to achieve the detector performance.

	Precision chambers		Trigger chambers	
	CSC	MDT	RPC	TGC
Number of chambers	32	1,194	1,136	1,584
Number of channels	31,000	370,000	385,000	322,000
Area covered (m <sup>2</sup> )	27	5,500	3,650	2,900

**Table 1:** Overview of the muon chamber instrumentation.

## 2. Monitored Drift Tubes

### 2.1 Design

The basic detection elements of the MDTs are aluminum tubes of 30 mm diameter and 400  $\mu\text{m}$  wall thickness, with a 50  $\mu\text{m}$  diameter W-Re(97:3) alloy wire. The tubes are operated with a non-flammable mixture of 93 % Ar and 7 % CO<sub>2</sub>, at 3 bar absolute pressure for reduced diffusion and ionization fluctuation. The wire is at a potential of 3080 V. The working point provides a linear space-time relation with a maximum drift time of 700 ns, and a small Lorentz angle. The amplification factor is set to be very low,  $2 \times 10^4$ , to minimize the ageing effect.

Each drift tube is read out at one end by a low-impedance current sensitive preamplifier. The preamplifier is followed by a differential amplifier, a shaping amplifier, and a discriminator (ASD). The output of the ASD gives the time over threshold information, the signal leading and trailing edge timing. The output of the shaping amplifier is also connected to an ADC, such that the charge-integrated signal can be used to correct the drift time measurement for time slewing. Eight ASD readout channels are packed, together with the ADCs, in a single custom CMOS processor. A signal from the ASD is fed into AMT (ATLAS Muon TDC) which measures the drift time with a resolution of better than 1 ns.

To improve the resolution beyond the single wire limit and to achieve an adequate redundancy for the pattern recognition, the MDTs are constructed from  $2 \times 4$  mono-layers of drift tubes for the inner and  $2 \times 3$  mono-layers for the middle and outer stations. A schematic drawing of the end-cap MDT chamber is shown in figure 3. The tubes are arranged on either side of the rigid support structures. According to the chamber location, the size of the MDT chamber is changed. The barrel MDT chambers form rectangles, while the end-cap ones have trapezoidal forms. The tube lengths vary from 810 mm to 6220 mm.

The structural components are three ‘cross plates’, to which the tube multi-layers are attached, and two ‘long beams’ connecting the cross plates. On the cross plates, an in-plane optical alignment system is mounted. This in-plane alignment scheme aims at monitoring the MDT wire displacements with an accuracy of 10  $\mu\text{m}$ . The displacements are



**Figure 2:** The barrel MDT chamber.

inferred from the relative movements of the cross plates, such as thermal expansion, small gravitational sag effects, and small deformations of chambers. For the in-plane alignment, four optical ‘RASNIK’ monitors are used. The RASNIK monitor is a simple imaging system consisting of an LED light ray, an illuminated MASK, a projection LENS, and a CCD sensor. Three dimensional positioning is obtained from an analysis of the mask image on the CCD, with accuracies of  $1 \mu\text{m}$  transverse to the optical axis and a few  $10 \mu\text{m}$  in the axial direction.

In order to measure the relative positions between the chambers, we introduce further optical alignment systems. We use the RASNIK again to monitor three MDTs stations and the adjacent chambers. Because the end-cap toroid cryostats prevent the implementation of a large number of projective light paths, the end-cap alignment system is based on a small number of projective reference bars connecting the chamber layers by an optical monitoring system. The bars are mechanically and thermally stable, and should be able to calibrate by themselves. An Active Test Program is underway at CERN H8 Test Facility not only for the alignment system but also for the integration and performance studies.

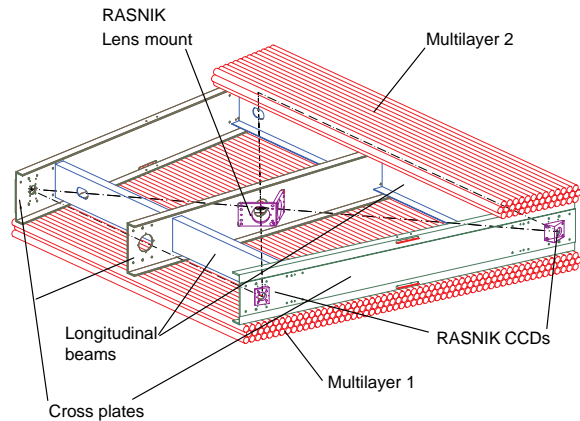


**Figure 3:** A schematic view of the end-cap MDT chamber.

## 2.2 Production

The tube productions and chamber assemblies started in July 2000. Nearly 40,000 drift tubes, more than 10 % of the total, corresponding to 80 chambers, have been produced (Figure 4). A total of 14 sites will participate in the production. To keep same quality at different sites, many strict quality controls are set. Major quality assurances for the tubes are; the wire position should be within  $\pm 25 \mu\text{m}$ , the wire tension should be  $350 \pm 15 \text{ g}$ , the tube length should be within  $\pm 0.5 \text{ mm}$ , the gas leak rate at 2 bar over pressure should be less than  $1 \times 10^{-8} \text{ bar}\cdot\text{l/s}$ , and the leak current at the 3400 V should be less than  $2 \text{ nA/m}$  (tube length). Up to now 3 % of the produced tubes have been rejected by these tolerance checks, mainly due to tube length(0.6%), gas leak(0.7%), wire tension(0.7%), and broken wire(0.6%).

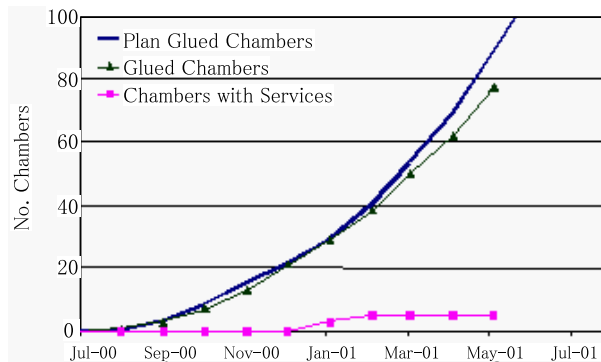


**Figure 4:** The production rate of MDT chambers.

Chamber assembly accuracy is essential to reach the requirements of track momentum resolution as well as chamber alignment monitoring. The target accuracy of the wire position is  $< 20\mu\text{m}$  in r.m.s.. Special tools are used for the fabrication of the MDT chambers; a precision jig installed on a granite table to achieve the mechanical tolerances, a lifting and rotating system for chamber manipulations, and a glue dispenser to perform the numerous gluing steps efficiently.

Using X-ray tomography examination we have measured wire positioning and check if the assemble procedure goes well or not at each site. Table 2 shows a result of the X-ray tomography examinations. Cosmic ray tests have been performed to check the MDTs chamber performance. An End-cap Inner Large (EIL) 4-layer chamber with the ATLAS electronics has been tested at the Boston site. A tube resolution of  $81\mu\text{m}$  was obtained.

Site	MDT type	Chambers	r.m.s. ( $\mu\text{m}$ )
Greece	BIS	2	8-12
Munich	BOS	2	8-9
Frascati	BML	1	10-13
Boston	EIL	1	12-17
Protvino	EOL	1	12-17
Nikhef	BOL	1	13-17
Roma	BIL	1	10-14
Seattle	EML	1	13-17
Michigan	EMS	1	15-21

### 3. Resistive Plate Chambers

#### 3.1 Design

The RPCs have simple mechanical structures with no wires and are therefore simple to manufacture. A narrow gas gap of 2 mm is formed by two parallel resistive Bakelite plates ( $\cong 10^{11}\Omega\text{ cm}$ ), separated by insulating spacers. The spacers are glued on both plates at 10 cm intervals. At all four edges same thickness spacers are used to seal the gas volume. The internal surfaces of the gas volume are coated with a thin uniform solid layer of linseed oil. This coating is done after the assembly of the gas volume. This makes a smooth surface, resulting in a reduction of the detector noise. The outside surfaces of the resistive plates are coated with graphite paints which are connected to a high voltage and a ground, making for a high, uniform electric field. These graphite electrodes are separated from the pick-up strips by  $200\mu\text{m}$  thick insulating PET films which are glued on both graphite

**Table 2:** Results of the MDT X-ray tomography. The r.m.s. means the  $\sqrt{dy^2 + dz^2}$  of the relative wire position.

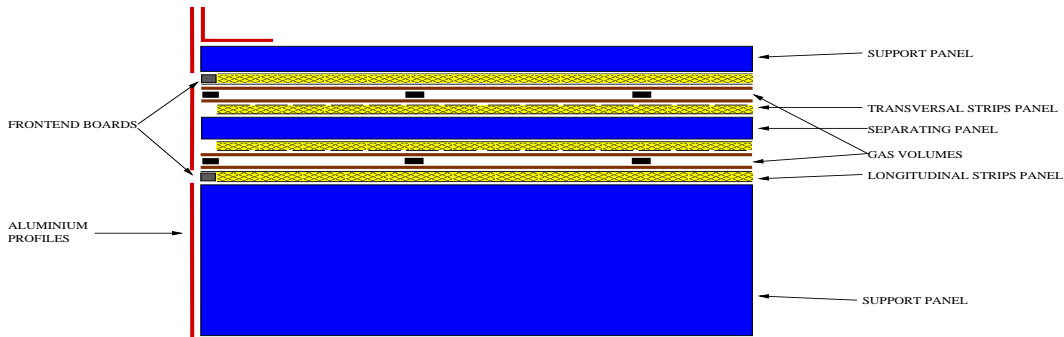


**Figure 5:** Mechanical structure of the RPC.

layers. The signal is read out by two orthogonal series of pick-up strips, which enable a two dimensional measurement. The strips parallel to the MDT wires provide the bending coordinate, and the other strips provide the second-coordinates. The readout strips are arranged with a pitch varying from 24 to 38 mm. The mechanical structure of the RPC is shown in figure 5. Each chamber is made from two detector layers and four readout strip panels. These elements are rigidly held together by two support panels and a separating panel. The size of the RPCs varies from 1060 mm to 2960 mm in width, from 310 mm to 1190mm in length.

The RPCs can be operated both in avalanche and streamer modes. In a high background environment, as in the LHC, the avalanche mode offers a higher rate capability and stable timing performance independent of the counting rate. The gas mixture is based on 96.7 % tetrafluoroethane ( $C_2H_2F_4$ ), which is a non-flammable and environmentally safe gas, and 3 % iso-butane ( $C_4H_{10}$ ). To suppress the streamer probability and to have a long term stable operation, 0.3 %  $SF_6$  is admixed. For the avalanche operation a high voltage of more than 10 kV is applied. In this condition, the streamer probability per muon signal is about 0.1 % and the rate capability is expected to be 1 kHz/cm<sup>2</sup>. A time resolution of 1.5 ns and an efficiency of more than 98 % including spacers and flames are typically achieved with this design.

A 15 months ageing test has been performed at the CERN X5 irradiation facility. After irradiation of 0.3 C/cm<sup>2</sup>, corresponding to 10 ATLAS years, we found that the RPC still had a rate capability of 200-300 Hz/cm<sup>2</sup>. We also obtained results that the cluster size and time resolution appeared not to be appreciably affected by ageing.

### 3.2 Production

Production of the RPCs are processed at five sites in Italy. To avoid duplication of tools and to have a higher efficiency in the production, work on each detector part is made at just one site. The gas volume and readout strip panels are produced at the General Tecnica Company. Some preparations for the readout panels are made at Naples University, and the front-end electronics are mounted on the readout panels in Roma-2. In Protvino the support panels and the Al profiles are produced. The unit assembly and the services mounting, such as the high voltage, low voltage, gas connector, and Faraday cage, are made in Lecce. A total

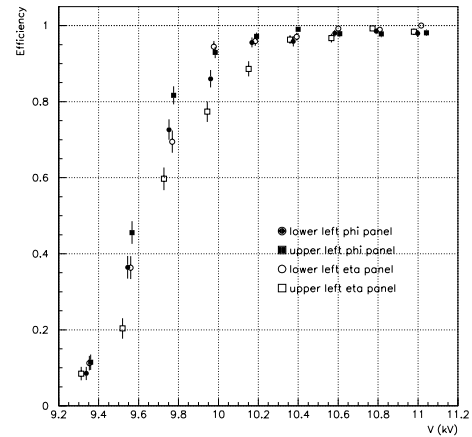


**Figure 6:** Efficiency plots with the cosmic rays.



**Figure 7:** The RPCs cosmic ray test station.

of 24 units (3 % of those to be produced) have been assembled in pre-production. This phase has been aimed to define all tools necessary for mass production and to finalize the services for the unit. Full production starts in October 2001, and the expected production rate is 3 units per day.

In order to examine the efficiency of the produced chambers three cosmic ray test stations have been build in Lecce, Roma2, and Naples. Each station allows a simultaneous test of 8 units and all stations are now operational. Figure 6 shows the efficiency curve of the high voltage dependence with the Barrel Outer Short (BOS) chamber, which was constructed in the pre-production.

## 4. Thin Gap Chambers

### 4.1 Design

The TGCs are designed in a way similar to the multi-wire proportional chambers, with the difference that the anode wire pitch is larger than the cathode-anode distance (figure 8). The main characteristics of the TGCs are the anode-cathode distance of 1.4 mm, the wire pitch of 1.8 mm, and the wire diameter of  $50 \mu\text{m}$ . The anode wire plane is sandwiched by support spacers between two cathode planes made of FR4 plates on which carbon graphite is deposited. On the backside of the cathode plane, etched copper strips provide an orthogonal readout to the wires readout, while on the other side, the copper plane is grounded. Using a highly quenching gas mixture of 55 %  $\text{CO}_2$  and 45 % n-pentane ( $\text{n-C}_5\text{H}_{12}$ ), this type of cell geometry allows for operation in a saturated mode. The operating high voltage is 3.0 kV. The electric field configuration and the small wire distance provide a short drift time and thus a good time resolution. An efficiency of more than 99 % can be achieved with the 25 ns gate.

Signals from the anode wires, arranged parallel to the MDT wires, provide the trigger information together with the readout strips arranged orthogonal to the wires. To form the trigger signal several anode wires are grouped together and fed to a common readout channel. The number of wires per group varies between 4 and 20, depending on the desired granularity as a function of the pseudorapidity. The readout strips serve to measure the second coordinates. The strip pitches also vary from 14 to 49 mm. All the TGCs have trapezoidal forms and are constructed in doublets and triplets. The seven TGC layers surrounding the middle MDT station are arranged in

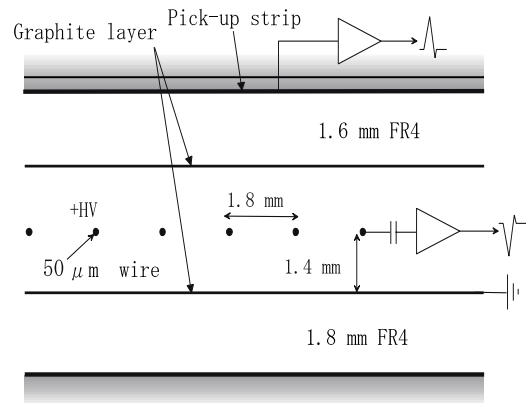


**Figure 8:** The TGC structure.

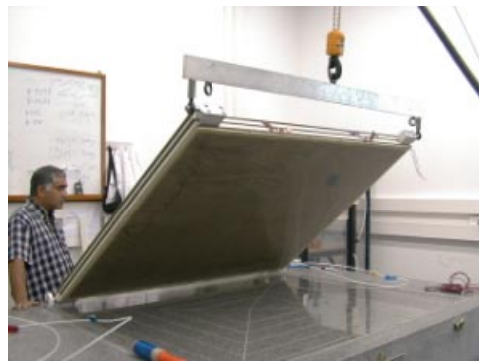


**Figure 9:** The TGC production.

one triplet and two doublets. In the doublet and triplet, the TGC layers are separated by a 20 mm thick paper honeycomb panel which makes a rigid mechanical structure for the chambers. On the outside, 5 mm thick paper honeycomb panels covered by 0.5 mm G-10 skins are attached to sustain the gas pressure.

## 4.2 Production

Three production sites will contribute to the TGCs mass production. Weizmann (Israel) intends to produce 576 doublets and 336 triplets. The production rate is about 10 chambers per week. Most of parts for the other sites are also prepared in Weizmann. In June 1999 mass production started, and up to now 200 doublets and 100 triplets have been completed. In KEK (Japan) 384 doublets and 96 triplets will be constructed. The production rate will be the same as that of Weizmann. We started pre-production in January 2001, and 40 triplets have been constructed. In December 2000 we performed a beam test to check the constructed chambers and to confirm our production procedure. Full production starts in October 2001. The other 192 doublets will be constructed in Shandong (China). The production rate will be about 5 chambers per week and production is expected to start in March 2002. Preparation is now in progress.

In the production procedure several quality controls are required. The carbon resistivity of the cathode plane should be  $1.0 \pm 0.5 \text{ M}\Omega / \square$  to keep a constant pulse height. Chamber flatness is important for such a large detector because mechanical deformation causes a change of the gas gap i.e. pulse height, which affects the time resolution. It is also important to check if a high voltage can be applied up to the appropriate value or not. Using  $\text{CO}_2$  or  $\text{CO}_2 + n\text{-pentane}$  gas a high voltage is applied to examine the leak current and stability of the chambers. These tests are repeated several times, before the TGCs closing, unit gluing, readout adapting, and shipping. As a final performance check the efficiency and time response of all produced TGCs will be tested with cosmic rays. Test benches are constructed in Technion (Israel), Tel-Aviv (Israel), and Kobe (Japan). Technion has already tested 50 triplets. Figure 10 shows a result of the TGC efficiency plot. Inefficient regions are the support spacers of the gas volume.

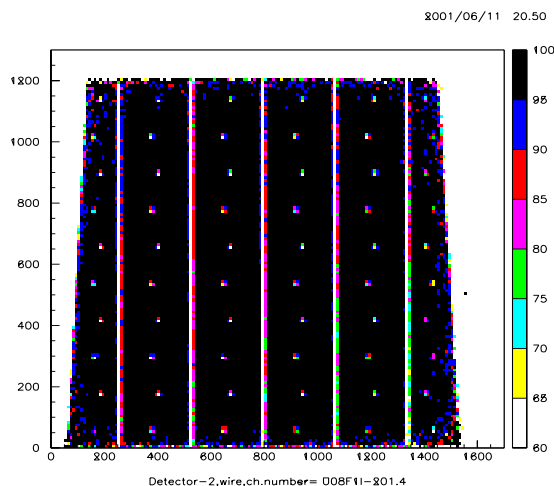


Figure 10: A TGC efficiency plot.

## 5. Trigger system

The ATLAS trigger system consists of three levels of online event selections [3]. Starting from a bunch crossing rate of 40 MHz, the rate of selected events must be reduced to about 100 Hz for permanent storage. The level-1 (LVL1) trigger provides an initial selection



based on reduced-granularity data from the subsets of the detectors. High- $P_T$  muons are identified using only the trigger chambers, the RPCs and TGCs. It is expected that LVL1 will reduce the rate to be less than 100 kHz. In the level-2 (LVL2) selection is performed using full-granularity data, which include the inner detectors, full calorimeters, and precision chambers information. Matching and isolation of the track-cluster are done by combining with these sub-detector information. The trigger rate should be reduced to be about 1 kHz in the LVL2. The last selection stage is performed in the event filter, where algorithms based on the offline code are applied.

### 5.1 Level-1 muon trigger

Bunch-crossing identification is essential to reconstruct the muon trajectory correctly, and to correlate the muon trigger to triggers from other sub-detectors. The trigger scheme is based on coincidences with a time resolution smaller than the bunch-crossing interval. Similar trigger schemes are used with the RPCs and TGCs (figure 11). The low- $P_T$  trigger uses only the coincidences of the RPC1 and RPC2 or of the TGC2 and TGC3, and the high- $P_T$  trigger utilizes all three stations. The  $\eta - \phi$  area is divided into sectors, 64 for the barrel and 144 for the end-caps. Two track candidates are selected at maximum in each sector. The information from all sectors is passed to the Muon Interface to the Central Trigger Processor, MUCTPI. The functions of the MUCTPI serve to solve the overlap, to calculate the total multiplicity, and to define the regions of interests (RoIs). The data are then sent to the central trigger processor.

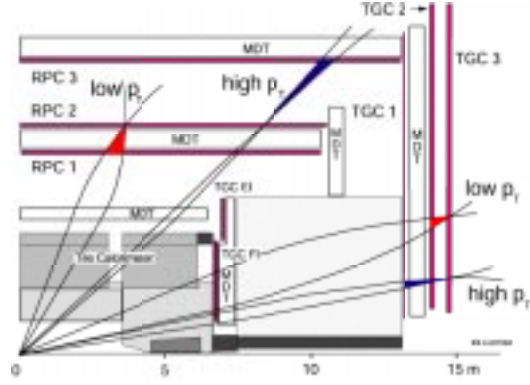


**Figure 11:** A schematic drawing of the Muon trigger scheme.

### 5.2 System structure

Figure 12 shows an overview of the data flow in the barrel trigger. A signal from the RPCs is sent to the amplifier-shaper-discriminator (ASD). The digitized signal is passed through the splitter board, and sent to the low- or high- $P_T$  Coincidence Matrix (CM). The CM ASIC serves a 3/4 majority coincidence for the low- $P_T$ , a 1/2 majority coincidence of the low- $P_T$  and the RPC3 for the high- $P_T$ . After the CM board, the data are sent to the Pad Logic board. The Pad board combines the  $\eta$  and  $\phi$ , solves the overlap, and selects the highest  $P_T$  candidate. The low- $P_T$  pad board generates the low- $P_T$  track candidate, and the high- $P_T$  pad board collects the overall result for the low-

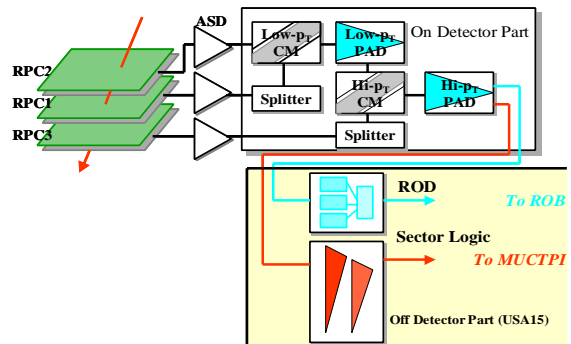


**Figure 12:** The barrel trigger system.

and high- $P_T$ . The combined information is sent to the Sector Logic board, which is located in the USA15 underground counting room. The Sector Logic is a Pipe-line processor of the low- $P_T$  filter, performs the Tile Calorimeter coincidence, solves the sector overlap, and generates the two highest  $P_T$  candidates. The trigger information is then sent to the MUCTPI. On the other hand, the read-out data are sent from the Read-Out Driver (ROD) to the Read-Out Buffers (ROB). For each part prototype boards have been designed and tested. A slice test including the control system is foreseen in late 2002.

A schematic drawing of the end-cap system is shown in figure 13. The Patch Panel (PP) performs the bunch crossing identification, and generates the fine delay and test pulse for the ASD. A local coincidence logic in two doublets or one triplet is done in the Slave Board (SLB). The trigger data are sent to the High- $P_T$  (HPT) board, which performs the high- $P_T$  coincidence in each R and  $\phi$  direction. The R,  $\delta R$ , and  $\phi$ ,  $\delta\phi$  information is then passed to the Sector Logic (SL). In the Sector Logic the R- $\phi$  coincidence is performed, and the two highest  $P_T$  tracks are selected. On the other hand, the read-out data are sent from the SLB to the Star Switch (SSW), which is a relay module. For all components prototype tests are in progress. The first slice test of the full system starts in September 2001, and a full system test before mass production is scheduled in 2002.

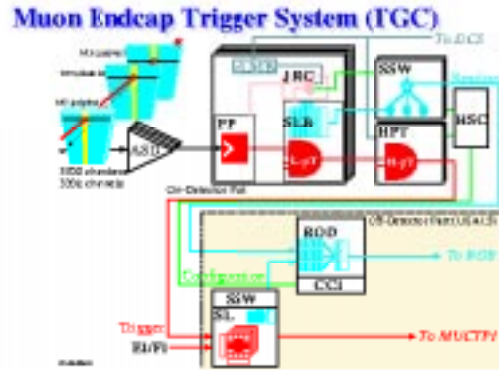


**Figure 13:** The end-cap trigger system.

## 6. Summary

By using the well established technologies the ATLAS Muon Spectrometer has been designed. We are convinced that this design will enable the ATLAS experiment to succeed. Production of the MDTs, RPCs, and TGCs started on schedule. In 3 years we should have built a large number of chambers. Many efforts are being made to get mass production under way, as well as to improve production quality. The designs of the trigger electronics are almost completed and we are entering a new phase of full system tests for the prototypes.

## References

- [1] The ATLAS Collaboration, DETECTOR AND PHYSICS Technical Design Report, CERN/LHCC/99-15, 25 May 1999.
- [2] The ATLAS Collaboration, MUON SPECTROMETER Technical Design Report, CERN/LHCC/97-2, 31 May 1997.
- [3] The ATLAS Collaboration, FIRST-LEVEL TRIGGER Technical Design Report, CERN/LHCC/98-14, 30 June 1998.